

The peak luminosity – peak energy correlation in GRBs

G. Ghirlanda^{1*}, G. Ghisellini¹, C. Firmani^{1,2}, A. Celotti³, Z. Bosnjak³

¹*Osservatorio Astronomico di Brera, via E. Bianchi 46, I-23807 Merate, Italy*

²*Instituto de Astronomía, U.N.A.M., A.P. 70-264, 04510, México, D.F., México*

³*SISSA/ISAS, via Beirut 4, I-34014 Trieste, Italy*

ABSTRACT

We derive the peak luminosity–peak energy ($L_{\text{iso}}-E_{\text{peak}}$) correlation using 22 long Gamma-Ray Bursts (GRBs) with firm redshift measurements. We find that its slope is similar to the correlation between the time integrated isotropic emitted energy E_{iso} and E_{peak} (Amati et al. 2002). For the 15 GRBs in our sample with estimated jet opening angle we compute the collimation corrected peak luminosity L_{γ} , and find that it correlates with E_{peak} . This has, however, a scatter larger than the correlation between E_{peak} and E_{γ} (the time integrated emitted energy, corrected for collimation; Ghirlanda et al. 2004), which we ascribe to the fact that the opening angle is estimated through the global energetics. We have then selected a large sample of 442 GRBs with pseudo–redshifts, derived through the lag–luminosity relation, to test the existence of the $L_{\text{iso}}-E_{\text{peak}}$ correlation. With this sample we also explore the possibility of a correlation between time resolved quantities, namely $L_{\text{iso}}^{\text{p}}$ and the peak energy at the peak of emission $E_{\text{peak}}^{\text{p}}$.

Key words: gamma rays: bursts – cosmology:observations

1 INTRODUCTION

Several correlations have been identified among the intrinsic properties of the (small) population of GRBs with measured redshifts z . In particular two spectral correlations have been recently discussed in the literature: i) the “Amati correlation” between the energy E_{peak} where most of the emission is radiated and the total emitted energy (isotropic equivalent) E_{iso} (Amati et al. 2002 - A02 hereafter; Lloyd & Ramirez–Ruiz 2002); ii) the “Ghirlanda correlation” between E_{peak} and the collimation–corrected energy E_{γ} (Ghirlanda, Ghisellini & Lazzati 2004 - GGL04 hereafter). It is important to notice that these correlations refer to the *time integrated* spectral properties of GRBs. This is true for both E_{peak} and for the spectral indices required to calculate the rest frame bolometric E_{iso} and E_{γ} .

However, time resolved spectral analysis of large samples of bursts (e.g. Ford et al. 1995; Preece et al. 2000; Ghirlanda, Celotti, Ghisellini 2002) have proved that the GRB spectrum evolves in time during the prompt emission phase. The spectral evolution is different among different GRBs (e.g. Ford et al. 1995) and not clearly linked to other GRB global parameters (e.g. duration, number of peaks, peak flux). This spectral evolution may be revealing of the time variation of the parameters of the radiative process(es) acting in GRBs (e.g. Liang & Kargatis 1996) and/or of the relativistic properties of the emitting outflow (e.g. Ryde & Petrosian 2002). In order to understand the origin of such correlations it is thus compelling to determine whether they are representing global

energetics characteristics or they hold for and are dominated by the time resolved spectral properties, as expected if determined by the emission process(es). One obvious possibility is to test them against the peak luminosity, well defined for all bursts with known z (e.g. Liang, Dai & Wu 2004).

This issue has been recently considered by Yonetoku et al. 2004 (Y04, hereafter). With a sample of 12 GRBs of known z they found that $E_{\text{peak}} \propto L_{\text{iso}}^{0.5}$. This correlation appeared to be tighter (but with similar slope) than the $E_{\text{peak}}-E_{\text{iso}}$ correlation, as originally found by A02. Note that the Y04 analysis adopts E_{peak} and the spectral indices of the time integrated spectrum and not the spectral properties at the peak flux.

In this Letter we first re–examine the $E_{\text{peak}}-L_{\text{iso}}$ correlation (i.e. the “Yonetoku correlation”) with an enlarged sample of 22 GRBs with spectroscopically measured z and published spectral properties. For 15 out of these 22 GRBs we have an estimate of their jet opening angle θ_j (GGL04). We can thus calculate the collimation corrected peak luminosity L_{γ} and verify if there exists the equivalent of the Ghirlanda correlation – namely L_{γ} replacing E_{γ} (Sec. 2). Then we consider a much larger sample of 442 GRBs with z estimated through the lag–luminosity correlation (Band, Norris & Bonnel 2004 - BNB04 hereafter) to test if the Yonetoku correlation still holds for this whole sample (Sec. 3). In Sec. 4, by means of this same sample, we also study the relation between $L_{\text{iso}}^{\text{p}}$ and $E_{\text{peak}}^{\text{p}}$, (i.e. using spectral parameters at the peak of the flux), to check whether this correlation is tighter than the Yonetoku one and we discuss the differences between the two. We find that the Ghirlanda correlation has a smaller scatter than the corresponding $E_{\text{peak}}-L_{\gamma}$

* E-mail: ghirlanda@merate.mi.astro.it

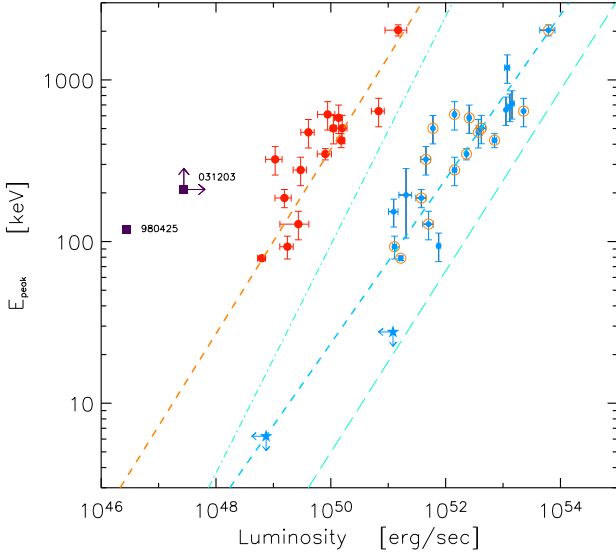


Figure 1. Rest frame peak energy $E_{\text{peak}} = E_{\text{peak}}^{\text{obs}}(1+z)$ versus the bolometric peak luminosity. Samples: GRBs with measured z listed in Tab. 1 (blue symbols) – upper/lower limits are excluded except for the 2 X-ray Flashes (stars), shown for comparison with Fig. 1 of GGL04; 15 GRBs with a firm measure of the jet break time (from Tab. 2 of GGL04) and hence of the jet opening angle θ_j (open yellow circles); same 15 GRBs once corrected for the $(1 - \cos \theta_j)$ collimation factor (red filled circles). Fits: best power-law fit to the $E_{\text{peak}}-L_{\text{iso}}$ correlation (dashed blue line); best fit $E_{\text{peak}}-L_{\gamma}$ correlation (dashed red line); the Amati correlation from 23 GRBs in GGL04 and GGF05 (long-dashed blue line) and the Ghirlanda correlation from GGL04 (dot-dashed blue line).

correlation. We give an interpretation of this result in Sec. 5 and draw our conclusions in the final Sec. 6.

In this paper we adopt a standard Λ CDM cosmology with $\Omega_{\Lambda} = 0.7$, $\Omega_{\text{M}} = 0.3$ and $h_0 = 0.7$.

2 THE $L_{\text{ISO}}-E_{\text{PEAK}}$ CORRELATION

The bolometric γ -ray luminosity can be defined once the prompt emission spectrum and the redshift z of the source are known. GRB spectra are typically described by the Band function $N(\alpha, \beta, E_{\text{peak}})$ (Band et al. 1993), parameterized by low and high energy power-laws (of photon indices α and β , respectively) and by peak energy E_{peak} in the νF_{ν} representation.

The burst emission varies on short timescales (e.g. Ramirez-Ruiz & Fenimore 1999) and no universal temporal profile describes the “zoology” of burst light curves (e.g. Norris et al. 1996). However, in most cases, a dominating peak, with flux Φ integrated in the observed energy band, can be identified in the prompt emission light curve. The rest frame, bolometric (e.g. $1-10^4$ keV), isotropic peak luminosity, including the redshift-energy band correction, follows straightforwardly. In Tab. 1 we report the peak luminosities of the 29 GRBs examined by GGL04, computed assuming the time integrated spectrum of each GRB (as from Tab. 1 in GGL04). No published spectrum was found for GRB 011121 (detected by *BeppoSAX*) and this is no further considered.

E_{peak} versus L_{iso} for these GRBs are shown in Fig. 1 (blue symbols). We omit upper/lower limits except for the two X-

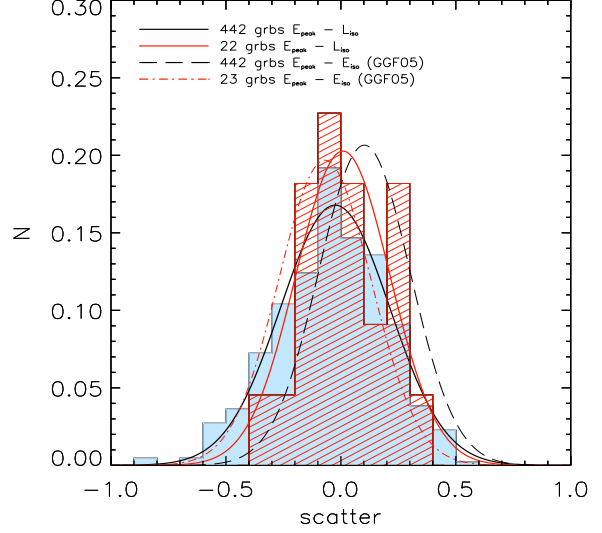


Figure 2. Distribution of the scatter of data points around their best fit correlations. Filled histogram: 442 GRBs with pseudo z (black crosses in Fig. 3) around their best powerlaw fit (solid blue line in Fig. 3), and Gaussian fit to this distribution (solid black line). Red hatched histogram: scatter of the 22 GRBs (blue symbols in Fig. 1) around their best fit line (long dashed blue line in Fig. 1), and the best Gaussian fit (red solid line). Also reported are the distributions of the scatter of the 23 and 442 GRBs of GGF05 with respect to their correlation in the $E_{\text{peak}}-E_{\text{iso}}$ plane.

ray Flashes with measured z . Note that the underluminous GRB 980425, associated with SN 1998bw, and GRB031203, associated with SN 2003lw, are major outliers for both the Yonetoku and the Amati correlations. The statistical results for the correlations are reported in Tab. 2, together with the corresponding best fitting power-law parameters (weighting for the errors on both coordinates). The highly significant correlation has slope similar to that found by Y04 with 12 GRBs. The distribution of the scatter measured along the correlation (i.e. the distances of the data points from the fitting line) of the 22 GRBs is shown in Fig. 2 (red-hatched histogram). A Gaussian fit (red solid line) to the distribution yields a scatter comparable to that of the 23 GRB in the $E_{\text{peak}}-E_{\text{iso}}$ plane (Ghirlanda, Ghisellini & Firmani (2005) - GGF05 - and black dashed line in Fig. 2).

For 15 out of the 22 GRBs listed in Tab. 1 we can correct their isotropic luminosity L_{iso} for the jet opening angle θ_j (Tab. 2 in GGL04), i.e. $L_{\gamma} = L_{\text{iso}}(1 - \cos \theta_j)$, with a corresponding error given by:

$$\left(\frac{\sigma_{L_{\gamma}}}{L_{\gamma}} \right)^2 = \left(\frac{\sigma_{L_{\text{iso}}}}{L_{\text{iso}}} \right)^2 + \left(\frac{\sigma_{\theta} \sin \theta_j}{1 - \cos \theta_j} \right)^2. \quad (1)$$

The red symbols in Fig. 1 define the $L_{\gamma}-E_{\text{peak}}$ correlation. Again all the statistical parameters are reported in Tab. 2. The scatter of the best fit correlation (dashed red line in Fig. 1) decreases with respect to that using L_{iso} – a trend similar to that found going from E_{iso} to E_{γ} (GGL04 and GGF05). As discussed by GGF05 in relation to the Amati correlation, also the scatter of the Yonetoku correlation found here can be interpreted as due to the distribution of jet opening angles. Note, however, that the scatter in the $E_{\text{peak}}-L_{\gamma}$

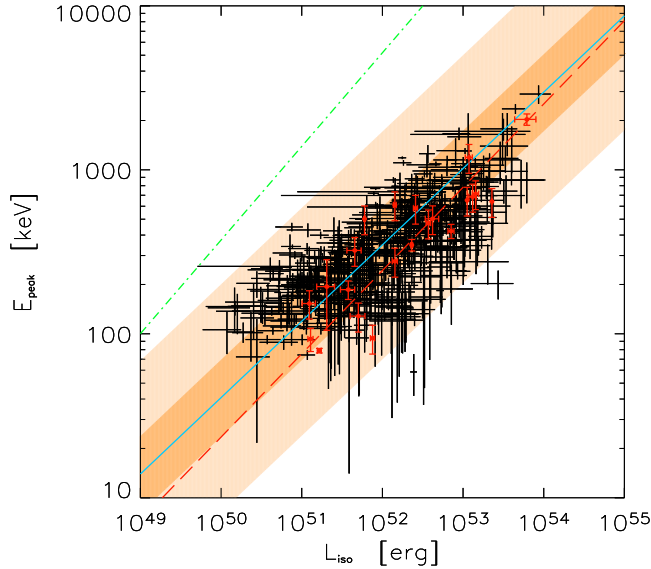


Figure 3. Rest frame peak energy E_{peak} versus peak luminosity L_{iso} . Samples: 442 GRBs with pseudo z defined in GGF05 (black crosses); 22 GRBs of Tab. 1 (red symbols). Fits: the powerlaw fit to the 442 black crosses (22 red symbols) is represented as solid blue line (dashed red line). The shaded regions show the 1σ and 3σ width of the dispersion of the black crosses around their best fit.

correlation is larger than that of the Ghirlanda correlation $E_{\text{peak}}-E_{\gamma}$. This fact will be discussed in Sec. 5.

3 THE PSEUDO REDSHIFTS SAMPLE

The original Amati correlation was found with 9 *BeppoSAX* GRBs with known z . Through a redshift independent test, Nakar & Piran (2004) and Band & Preece (2005) claimed that the larger BATSE sample is inconsistent (at 40% and 88% level, respectively) with the original Amati correlation. However, GGF05 (see also GGL04) have confirmed the above correlation (but finding a larger scatter) using a sample of 23 bursts with measured z as well as using a sample of hundreds GRBs with pseudo z . An even more general conclusion, i.e. the consistency of the above correlations with the entire BATSE long bursts sample, has been derived by Bosnjak et al. (2005).

The same test of GGF05 can be performed for the $E_{\text{peak}}-L_{\text{iso}}$ correlation found in Sec. 2. More importantly, it is worth to investigate if its scatter and slope change using this much larger sample. To this aim we consider the same sample defined in GGF05, which comprises 442 GRBs with pseudo z [estimated by BNB04 through the lag-luminosity relation] and known peak energy of the *time integrated spectrum* (found by Y04). Since the photon spectral indices are not given in Y04, in order to compute L_{iso} we assume typical values, i.e. $\alpha = -0.8$, $\beta = -2.5$ (see e.g. Preece et al. 2000).

In Fig. 3 we show these 442 GRBs (black crosses) in the rest frame E_{peak} vs L_{iso} plane, and in Fig. 2 we show the distribution of the scatter of the 442 points around this correlation (blue histogram in Fig. 2) together with its Gaussian fit (black solid line in Fig. 2). This scatter is only slightly larger than that defined by the 22 GRBs

with measured z (red-hatched histogram and red solid line in Fig. 2), and the slope of the correlations is similar (see Tab. 2).

For comparison with what found for the Amati correlation by GGF05, Fig. 2 also reports the scatter distribution for the $E_{\text{peak}}-E_{\text{iso}}$ relation with the same samples of 23 and 442 GRBs (dot dashed red and black dashed line, respectively). As already mentioned, the scatter of the Yonetoku correlation for the 442 GRBs can be interpreted as due to the distribution of the jet opening angles. Assuming that the $E_{\text{peak}}-L_{\gamma}$ correlation has a smaller scatter than the Yonetoku one, we can estimate the jet opening angle distribution for the 442 GRBs: we find a lognormal with a peak at $\theta \sim 5^\circ$, i.e. consistent with that found in GGF05.

4 THE $E_{\text{PEAK}}^{\text{P}}-L_{\text{ISO}}^{\text{P}}$ CORRELATION

To the aim of investigating the spectral correlations at the peak of the prompt emission, the most correct approach would be to analyze the spectrum of each GRB, time resolved at the burst peak. This would allow to derive a peak spectral energy $E_{\text{peak}}^{\text{P}}$ and a luminosity (from the spectrum at the peak of the burst) $L_{\text{iso}}^{\text{P}}$ which, in general, might be different from the analogous integrated quantities.

Given that the GRBs listed in Tab. 1 were detected by different satellites and that the data are public only for BATSE, we can investigate the $E_{\text{peak}}^{\text{P}}-L_{\text{iso}}^{\text{P}}$ correlation only with the sample of 442 GRBs with pseudo z . For these, in fact, Mallozzi et al. (1998) provide the spectral parameters of the peak spectrum, derived by integrating the GRB signal for ~ 2 sec around the light curve peak, and BNB04 report the peak flux corresponding to the same peak spectrum.

The sample of 442 GRBs allows a direct comparison with the results obtained in GGF05. However, we here exclude a few bursts because either their $E_{\text{peak}}^{\text{P}}$ is below the BATSE ~ 30 keV energy threshold (7 cases) or $E_{\text{peak}}^{\text{P}}$ is not constrained by the spectral fit (11 cases with $\beta > -2$). We report in Fig. 4 the remaining 424 GRBs with pseudo- z . Also in this case we find a strong correlation with a scatter consistent with that obtained adopting L_{iso} (Sec. 3), and a slightly flatter slope. In other words, the peak energy and luminosity at the peak are correlated, but the correlation is not significantly tighter than the Yonetoku correlation (see Tab. 2).

5 THE ORIGIN OF THE SCATTER OF THE $E_{\text{PEAK}}-L_{\gamma}$ CORRELATION

In Sec. 2 we have derived the equivalent of the Ghirlanda correlation with the peak luminosity, i.e. $E_{\text{peak}}-L_{\gamma}$. This correlation (red symbols in Fig. 1) has a scatter a factor 1.7 larger than that of the Ghirlanda correlation (for the same GRBs). This implies that time integrated quantities correlate better than time resolved (“instantaneous”) ones at the peak of the emission.

One possible reason can be envisaged by comparing the peak luminosity L_{iso} as a function of the isotropic energy E_{iso} for the sample of 15 GRBs of measured z and jet opening angle (Fig. 5). The two quantities are correlated, but with a considerable scatter, which is comparable to the scatter of the $E_{\text{peak}}-L_{\gamma}$ correlation: in the insert of Fig. 5 the Gaussian fits to the scatter distributions of the $L_{\text{iso}}-E_{\text{iso}}$ ($\sigma = 0.33$, black line) and the $E_{\text{peak}}-L_{\gamma}$ correlation ($\sigma = 0.31$, red line) are reported. Note that in this case the scatter corresponds to the ‘horizontal’ distance of the points from the fitting line.

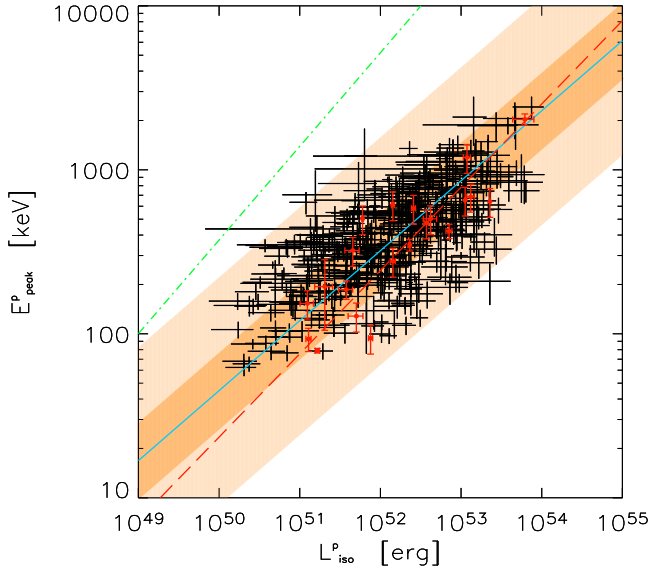


Figure 4. Rest frame peak energy E_{peak}^P versus peak luminosity L_{iso}^P for the sample of 424 GRBs with pseudo z . The red symbols represent the 22 GRBs of Tab. 1 (reported for comparison although their peak energy and luminosity are derived assuming their time average spectrum, see Sec. 2). The solid blue line (dashed red line) is the powerlaw fit to the 442 black crosses (22 red symbols). The shaded regions represent the 1σ and 3σ width of the dispersion of the black crosses around their best fit.

The smaller scatter of the Ghirlanda correlation with respect to the $E_{\text{peak}}-L_\gamma$ one can be then ascribed to the fact that L_γ has a larger spread with respect to E_γ . Interestingly, this might be related to E_γ being a time integrated quantity, better representing the total kinetic energy of the fireball, which is the quantity involved in the derivation of the jet opening angle (e.g. Sari, Piran & Halpern 1999). On the contrary, L_γ might be more subject to local and temporal fluctuations in the fireball, not representative of the global energetics.

6 CONCLUSIONS

We derived the $E_{\text{peak}}-L_{\text{iso}}$ correlation with the current largest available sample of 22 GRBs with known z and well determined spectral properties (GGL04). This correlation has a slope 0.51, i.e. similar to that proposed by Y04, although its scatter is much larger than they originally found with 12 GRBs. The scatter is instead comparable with what GGF05 found for the Amati correlation using the same sample of GRBs. Using the 442 GRBs with pseudo- z we still find a strong correlation, with similar scatter and slightly flatter slope than those found with the 22 GRB of measured z .

We then considered the robustness of correlations for quantities calculated at the peak of the emission, with respect to time integrated properties. The former, in particular E_{peak}^P vs L_{iso}^P , results in a correlation equally tight to that involving integrated quantities.

Correcting L_{iso} for collimation, we found that the corresponding $E_{\text{peak}}-L_\gamma$ correlation has a slope flatter than the Ghirlanda correlation (0.57 vs 0.7) and a larger scatter (0.17 vs 0.1). The larger scatter might be ascribed to the fact that the peak luminosity is less representative of the global energetics of the burst, which in turn is

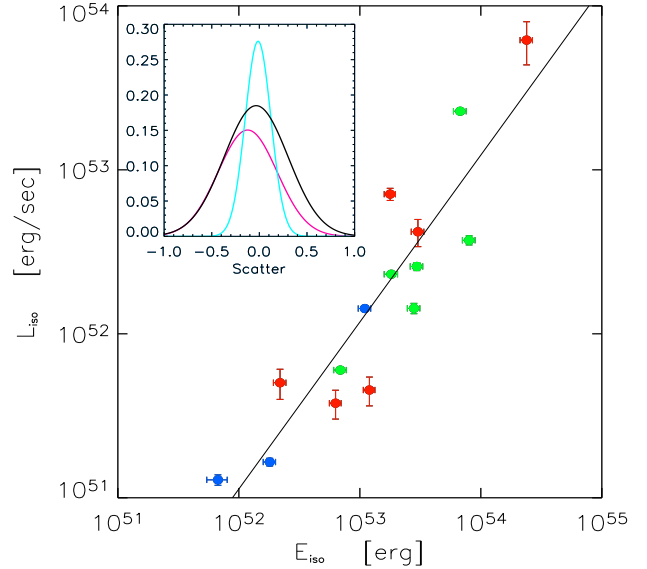


Figure 5. Peak isotropic luminosity L_{iso} versus isotropic energy E_{iso} for the 15 GRBs with measured z and jet angle. Different colors represent different z ranges: $z < 0.7$ (blue), $0.7 < z < 1.55$ (green), $z > 1.55$ (red). The solid line (with slope 1.0) shows the least square fit. The insert reports the Gaussian fit to the scatter of the data points around this correlation (black line), compared to the scatter (red line) of the 15 GRBs with known angle (red points in Fig. 1) around the $E_{\text{peak}}-L_\gamma$ correlation. Also represented (blue line) is the scatter of the same 15 points in the $E_{\text{peak}}-E_{\text{iso}}$ plane around the Ghirlanda correlation.

adopted to represent the total kinetic energy of the fireball and thus estimate the jet opening angle (e.g. Sari et al. 1999).

ACKNOWLEDGMENTS

The Italian MIUR and INAF are acknowledged for funding by G. Ghirlanda, G. Ghisellini (Cofin grant 2003020775.002), AC and ZB.

REFERENCES

- Amati, L. et al. 2002, A&A, 390, 81
- Band, D.L., et al. 1993, ApJ, 413, 281
- Band, D.L. & Preece, R.D., 2005, subm. to ApJ (astro-ph/0501559) (BP05)
- Band, D.L., Norris, J.P. & Bonnell, J.T., 2004, ApJ, 613, 484 (BNB04)
- Bosnjak, Z., Celotti, A., Longo, F., Barbiellini, G., 2005, subm. to MNRAS (astro-ph/0502185)
- Firmani, C., Ghisellini, G., Ghirlanda, G. & Avila-Reese, V., 2005 MNRAS (Letters), in press (astro-ph/0501395)
- Ford L. A. et al., 1995, ApJ, 439, 307
- Frontera, F. et al., 2001, ApJ 550, L47
- Ghirlanda, G., Celotti A. & Ghisellini G., 2002, A&A, 393, 409
- Ghirlanda, G., Ghisellini, G. & Lazzati, D., 2004, ApJ, 616, 331 (GGL04)
- Ghirlanda, G., Ghisellini, G. & Firmani, C., 2005, subm. to MNRAS, (astro-ph/0502186) (GGF05)
- Jimenez, R., Band, D.L. & Piran, T., 2001, ApJ, 561, 171
- Liang, E.P. & Kargatis, V.E., 1996, Nature, 381, 49
- Liang E., Dai Z. & Wu X. F., 2004, ApJ, 606, L29
- Lloyd-Ronning, N.M. & Ramirez-Ruiz E., 2002, ApJ, 576, 101.

GRB		Φ_{peak} phot/cm ² sec	Φ_{peak} erg/cm ² sec	band (keV)	$\Phi(1-10^4 \text{ keV})$ erg/cm ² sec	L_{iso} erg/sec
970228	S(1)	...	(3.7±0.8)E-6	40-700	7.4E-6	(1.6±0.3)E52
970828	B(2)	...	(5.93±0.34)E-6	30-10 ⁴	5.5E-6	(2.6±0.2)E52
971214	S(1)	...	(0.68±0.07)E-6	40-700	1.2E-6	(1.3±0.1)E53
980425	B(3)	0.4±0.1	...	50-300	1.7E-7	(2.7±0.35)E46
980613	S(1)	...	(0.16±0.04)E-6	40-700	3.1E-7	(2.0±0.51)E51
980703	B(3)	2.39±0.06	...	50-300	1.3E-6	(6.0±0.2)E51
990123	S(1)	...	(17.0±5.0)E-6	40-700	3.7E-5	(6.2±1.8)E53
990506	B(3)	18.58±0.13	...	30-500	1.1E-5	(1.1±0.6)E53
990510	S(1)	...	(2.47±0.21)E-6	40-700	4.1E-6	(7.1±0.6)E52
990705	S(1)	...	(3.7±0.1)E-6	40-700	6.7E-6	(2.3±0.1)E52
990712	S(4)	4.1±0.3	...	40-700	1.9E-6	(1.3±0.1)E51
991216	B(3)	67.5±0.2	...	50-300	4.2E-5	(2.27±0.01)E53
000131	B(3)	7.5E-7	(1.43±0.16)E53
000214	S(1)	...	(4.0±0.2)E-6	40-700	>9.9E-6	>6.2E51
000911	I(5)	...	(2.0±0.2)E-5	15-8000	2.0E-5	(1.2±0.2)E53
010222	S(1)	...	(8.6±0.2)E-6	40-700	>2.3E-5	>3.2E53
010921	H(7)	3.19±0.3	...	50-300	1.7E-6	(1.2±0.2)E51
011211	S(6)	...	(5.0±1.0)E-8	40-700	1.1E-7	(3.8±0.8)E51
020124	H(7)	9.38±1.77	...	2-400	4.6E-7	(4.2±0.8)E52
020405	I(5)	...	(5.0±0.2)E-6	15-2000	6.8E-6	(1.4±0.1)E52
020813	H(7)	32.31±2.07	...	2-400	4.1E-6	(3.7±0.2)E52
020903X	H(7)	2.78±0.67	...	2-400	9.1E-9	<2.4E51
021211	H(7)	29.97±1.74	...	2-400	1.4E-6	(7.6±0.5)E51
030226	H(7)	...	(1.2±0.2)E-7	30-400	1.6E-7	(4.5±1.0)E51
030328	H(7)	11.64±0.85	...	2-400	9.7E-7	(1.4±0.1)E52
030329	H(7)	450.88±24.68	...	2-400	2.1E-5	(1.7±0.1)E51
030429	H(7)	3.79±0.79	...	2-400	8.7E-8	(5.0±1.0)E51
030723X	H(7)	2.10±0.41	...	2-400	3.7E-8	<1.2E51
031203	I(8)	...	2.4E-7	20-200	>9.6E-9	>2.8E47

Table 1. Peak fluxes and bolometric luminosities for GRBs with measured z (in GGL04). S=BeppoSAX, B=Batse, I=Integral, H=Hete-II. Photon peak fluxes or energy peak fluxes with references (col. 2) and corresponding observed energy band (col. 5). References: (1) Amati et al. 2002; (2) Yonetoku et al. 2004; (3) 4th Batse catalog; (4) Frontera et al. 2001; (5) Price et al. 2002; (6) Piro et al. 2004; (7) Sakamoto et al. 2004. (8) Sazonov et al. 2004.

Correlation	N	r_s	P	r_z	A	S_o	δ	$\chi^2/\text{d.o.f.}$	μ	σ
$E_{\text{peak}}-L_{\text{iso}}$	22	0.87	8.5×10^{-8}	0.83	2.00 ± 0.05	7.4×10^{51}	0.50 ± 0.02	127/20	0.01	0.20
$E_{\text{peak}}-L_{\gamma}$	15	0.88	1.6×10^{-5}	0.85	2.56 ± 0.12	4.3×10^{49}	0.57 ± 0.03	49.6/13	0.04	0.17
$E_{\text{peak}}-E_{\gamma}$	15	0.95	2.8×10^{-8}	0.94	2.62 ± 0.15	4.2×10^{50}	0.70 ± 0.05	16.5/13	-0.07	0.10
$E_{\text{peak}}-L_{\text{iso}}^{\text{p}}$	442	0.71	1.6×10^{-69}	0.7	4.36 ± 0.04	1.6×10^{52}	0.47 ± 0.01	4171/440	-0.02	0.23
$E_{\text{peak}}^{\text{p}}-L_{\text{iso}}^{\text{p}}$	424	0.66	5.1×10^{-65}	0.65	3.80 ± 0.06	1.6×10^{52}	0.43 ± 0.01	4154/422	0.05	0.23

Table 2. Statistical results. N : Number of objects; r_s : Spearman correlation coefficient; P : Chance Probability; r_z : Partial correlation coefficient subtracting the effect of z (e.g. Wall & Jenkins 2003); A , S_o and Ω : Linear Fit Normalization, Scaling and Slope, i.e.: $(E_{\text{peak}}/100 \text{ keV}) = A(S/S_o)^{\delta}$; μ and σ : Gaussian fit parameters.

Mallozzi, R.S., et al., 1998, in Gamma Ray Bursts, 4th Huntsville Symposium. AIP conf. proceedings 428, eds. C. Meegan, R. Preece and T. Koshut (AIP: Woodbury, NY), 273
Nakar, E. & Piran, T., 2004, subm. to ApJ, astro-ph/0412232 (NP04)
Norris, J.P. et al. 1996, ApJ, 301, 213
Piro, L. et al., 2004, ApJ, in press (astro-ph/0412589)
Preece, R. et al., 2000, APJS, 126, 19
Price, R. et al., 2002, ApJ, 573, 85
Ramirez-Ruiz, E. & Fenimore, E., 1999, A&A, 138, 521
Ryde, F. & Petrosian, V., 2002, ApJ, 578, 290
Sakamoto, T. et al., 2004, ApJ subm. (astro-ph/0409128)
Sari, R., Piran, T., & Halpern, J.P., 1999, ApJ 524, L43
Sazonov, S. Yu.; Lutovinov, A. A. & Sunyaev, R. A., 2004, Nature, 430, 646

Yonetoku, D. et al. 2004, ApJ, 609, 935 (Y04)
Wall, J. V. & Jenkins C. R., 2003, Practical Statistics for Astronomers, Cambridge University Press.